Free Radical Research, August 2005; 39(8): 825–836

Characterization of the high-resolution ESR spectra of superoxide radical adducts of 5-(diethoxyphosphoryl)-5-methyl-1-pyrroline *N*-oxide (DEPMPO) and 5,5-dimethyl-1-pyrroline *N*-oxide (DMPO). Analysis of conformational exchange

SERGEY DIKALOV[1,2], JINJIE JIANG[1], & RONALD P. MASON[1]

[1]*Laboratory of Pharmacology and Chemistry, National Institute of Environmental Health Sciences, National Institutes of Health, Research Triangle Park, NC 27709, USA, and* [2]*Division of Cardiology, Emory University School of Medicine, 1639 Pierce Drive, SMRB 319, Atlanta, GA 03022, USA*

Accepted by Professor Dr B. Kalyanaraman

(Received 8 March 2005; in revised form 4 April 2005)

Abstract

It has been previously reported that the spin trap 5-(diethoxyphosphoryl)-5-methyl-1-pyrroline *N*-oxide (DEPMPO) can form stable radical adducts with superoxide radical. However, the presence of diastereomers of DEPMPO radical adducts and the appearance of superhyperfine structure complicates the interpretation of the ESR spectra. It has been suggested that the superhyperfine structure in the ESR spectrum of DEPMPO/˙OOH is a result of conformational exchange between conformers. The analysis of the temperature dependence of the ESR spectrum of DEPMPO/˙OOH and of its structural analog DMPO/˙OOH have demonstrated that both ESR spectra contain exchange effects resulting from conversion between two conformers. Computer simulation calculates a conformer lifetime on the order of 0.1 μs for DMPO/˙OOH at room temperature. However, temperature dependence of the ESR spectrum of DEPMPO/˙OOH suggests that superhyperfine structure does not depend on the conformational exchange. We have now found that the six-line ESR spectrum with superhyperfine structure should be assigned to a DEPMPO-superoxide-derived decomposition product. Therefore, ESR spectra previously assigned to DEPMPO/˙OOH contain not only the two diastereomers of DEPMPO/˙OOH but also the decomposition product, and these spectra should be simulated as a combination of four species: two conformers of the first diastereomer, one conformer of the second diastereomer and the superoxide-derived decomposition product. The presence of four species has been supported by the temperature dependence of the ESR spectra, nucleophilic synthesis of radical adducts, and isotopic substitution experiments. It is clear that to correctly interpret DEPMPO spin trapping of superoxide radicals, one must carefully consider formation of secondary radical adducts.

Keywords: *Spin trap, DEPMPO, DMPO, superoxide radical, radical adduct, oxygen-17*

Abbreviations: *DEPMPO, 5-(diethoxyphosphoryl)-5-methyl-1-pyrroline N-oxide; DMPO, 5,5-dimethyl-1-pyrroline N-oxide; M4PO, 3,3,5,5-tetramethyl-1-pyrroline-N-oxide*

Introduction

Superoxide radicals play a key role in oxidative damage under different pathophysiological conditions [1,2]. However, they are very short-lived species, and in most cases, the sensitivity of ESR spectroscopy is insufficient for direct detection. Because, longer-lived radical adducts can be produced by reacting these short-lived radicals with spin-traps (Scheme 1) [3,4], the spin-trapping technique is uniquely important in the study of the superoxide radicals [5,6].

Correspondence: R. P. Mason, Laboratory of Pharmacology and Chemistry, National Institute of Environmental Health Sciences, National Institutes of Health (NIEHS/NIH), Research Triangle Park, NC 27709, USA. Tel: 1 919 541 3910. Fax: 1 919 541 1043.
E-mail: mason4@niehs.nih.gov

ISSN 1071-5762 print/ISSN 1029-2470 online © 2005 Taylor & Francis Group Ltd
DOI: 10.1080/10715760500155688

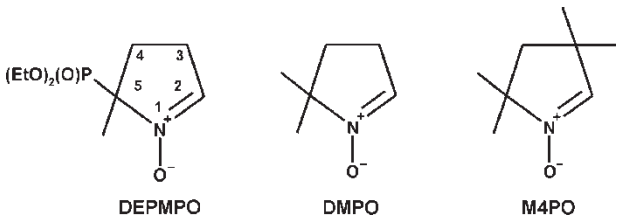

Scheme 1. Chemical structures of the spin traps.

Unfortunately, the detection of the superoxide radicals has been very limited by the short lifetimes of the radical adducts [5,6]. It has been reported that the spin trap 5-(diethoxyphosphoryl)-5-methyl-1-pyrroline *N*-oxide (DEPMPO) forms a very stable superoxide radical adduct with a characteristic ESR spectrum [7–9]. However, analysis of these spectra is complicated by the presence of two chiral centers at the second and fifth positions (Scheme 1), producing two chemically distinguishable diastereomers [10].

Moreover, it has been suggested that the ESR spectrum of DEPMPO/˙OOH exhibits linewidth alternation because of exchange between the two conformers [8,9], complicating the analysis of the ESR spectra even further. The appearance of superhyperfine structure in the ESR spectrum of DEPMPO/˙OOH was associated with linewidth alternation. In this work, we have examined the temperature dependence of the ESR spectra of DMPO/˙OOH and DEPMPO/˙OOH and determined the effect of conformational exchange, which results in the appearance of asymmetry in the line shape but does not affect the superhyperfine structure.

We also report here that ESR spectra previously assigned to DEPMPO/˙OOH are likely to contain an additional superoxide-derived decomposition product. This product has a six-line ESR spectrum with superhyperfine structure that is not present in the signals from the diastereomers. We suggest that ESR spectra previously assigned to DEPMPO/˙OOH consist of the two diastereomers of DEPMPO/˙OOH plus the newly identified decomposition product and, therefore, should be simulated as a combination of four species: two conformers of the first diastereomer (80%), the second diastereomer (13%) and a superoxide-derived decomposition product (7%). The presence of four species has been supported by the temperature dependence of the ESR spectra, nucleophilic synthesis of radical adducts, and isotopic substitution experiments. Clearly, the correct interpretation of spin trapping of superoxide by DEPMPO needs careful consideration of the formation of secondary radical adducts.

Materials and methods

The spin trap 5-(diethoxyphosphoryl)-5-methyl-1-pyrroline *N*-oxide (DEPMPO) was obtained from OXIS (Portland, OR) and stored at −70°C. Superoxide dismutase (SOD) (EC 1.15.1.1) was acquired from Roche (Indianapolis, IN). Spin traps 5,5-dimethyl-1-pyrroline *N*-oxide (DMPO) and 3,3,5,5-tetramethyl-1-pyrroline-*N*-oxide (M4PO) were supplied by Alexis Corporation (Läufelfingen, Switzerland). DMPO was vacuum-distilled twice at room temperature and stored under nitrogen at −70°C. Diethylenetriaminepentaacetic acid (DTPA), manganese SOD (EC 1.15.1.1), and xanthine were obtained from Sigma (St Louis, MO). Xanthine oxidase was purchased from Roche Molecular Biochemicals (Indianapolis, IN). Hydrogen peroxide was from Fisher Scientific (Fair Lawn, NJ).

Superoxide radical generation

The xanthine oxidase superoxide-generating system [11] contained xanthine oxidase, xanthine (0.5 M), and DTPA (0.2 mM) in 50 mM sodium phosphate buffer (pH 7.4) in the presence of 0.9% NaCl. The rate of superoxide radical generation was determined by the cytochrome *c* assay [12].

ESR experiments

All ESR samples were placed in a 10 mm flat cell (Wilmad, NJ). Spin trapping of superoxide was carried out in 50 mM sodium phosphate buffer (pH 7.4) with 0.9% NaCl. In order to inhibit iron-catalyzed reactions, DTPA (200 μM) was added to all samples. ESR spectra were recorded using an ELEXSYS ESR spectrometer (Bruker BioSpin, MA) and an SHQ microwave cavity.

In the experiments with $^{17}O_2$ and analysis of decay of the radical adducts by subtraction of ESR spectra, DEPMPO radical adducts were generated by the xanthine oxidase superoxide-generating system with slow flow for 2 min through the flat cells. Then the reaction was stopped by purging the flat cell with argon or nitrogen gas to remove oxygen from the sample, thereby, stopping the formation of new DEPMPO superoxide adduct and avoiding the line broadening by oxygen concentration.

For DEPMPO samples, eight consecutive ESR spectra were recorded, where each spectrum was scanned with the following settings: field sweep, 120 G; microwave frequency, 9.78 GHz; microwave power, 20 mW; modulation amplitude, 0.2 G; conversion time, 20.5 ms; time constant, 20.5 ms; receiver gain, 1×10^5 (74 dB); number of points, 4096; number of scans, 8. The ESR instrumental settings for experiments with DMPO and M4PO were as follows: field sweep, 80 G; microwave frequency, 9.78 GHz; microwave power, 20 mW; modulation amplitude, 0.5 G; conversion time, 167 ms; time constant, 167 ms; receiver gain, 1×10^5; number of scans, 4; and number of points, 1024. ESR spin-trapping experiments were repeated at least three times.

Slow flow experiment

In order to minimize decay of the radical adducts and obtain high-resolution ESR spectra with good signal-to-noise ratio, we have acquired DEPMPO radical adducts in the slow flow experiments. The solutions from two syringes were mixed in a mixing chamber using a Harvard Apparatus PHD 2000 pump. The mixed solution was flowed through a Bruker AquaX sample cell installed in an SHQ microwave cavity. Spin trapping of superoxide radical was studied by mixing a solution of xanthine oxidase with xanthine plus DMPO or DEPMPO. Formation of radical adducts was studied with various flow rates (0.1–3 ml/min) in order to achieve maximum ESR signals. The effect of superoxide dismutase was tested by adding Mn-SOD (50 U/ml) to both solutions. The ESR instrumental settings for flow experiments with the spin trap DEPMPO were as follows: field sweep, 120 G; microwave frequency, 9.78 GHz; microwave power, 20 mW; modulation amplitude, 0.2 G; conversion time, 83 ms; time constant, 83 ms and receiver gain, 1×10^5 (74 dB).

Simulation of ESR spectra

Computer simulation of experimental ESR spectra was used for the calculation of hyperfine coupling constants. Programs for the simulation of ESR spectra and the spin-trap database are readily available to the public through the Internet (http://epr.niehs.nih.gov/). The details of this computer simulation program have been described elsewhere [13]. Hyperfine coupling constants are expressed as an average of ESR parameters obtained from computer simulations using at least three experimental spectra, which provides precision of not less than 0.05 G. A special simulation was written in C++ to generate ESR spectra with exchange effects based on modified Block equations.

Results

Effect of temperature on ESR spectra of DMPO/˙OOH

Previously, it had been proposed that the super-hyperfine structure in the ESR spectrum of DEPMPO/˙OOH was the result of conformational exchange between conformers of one of the DEPMPO/˙OOH diastereomers [8,9]. This exchange phenomenon is one of the most fascinating effects that change EPR line shape and linewidth. It takes place when chemical or conformational exchange proceeds between two or more free radicals on the ESR time scale. In order to gain insight into the effect of conformational exchange on the ESR spectrum of DEPMPO/˙OOH, we analyzed the temperature dependence of the ESR spectrum of its structural analog DMPO/˙OOH (Figures 1–3).

At 4°C, DMPO/˙OOH produced an asymmetric ESR spectrum that was transformed to a highly symmetric spectrum at 67°C (Figure 1A and E). Simulation of the spectrum at 4°C revealed the presence of two conformers of DMPO/˙OOH (Figure 1C and D). At 67°C, fast exchange between these conformers led to a highly symmetric spectrum of DMPO/˙OOH with a hyperfine coupling constant of 1.22 G on the γ-proton (Figure 1G).

Recently, it has been suggested that DMPO/˙OOH has no hyperfine coupling constant from the γ- proton but is rather a result of two conformers of DMPO/˙OOH in slow exchange with distinctly different hyperfine coupling constants from the β-proton [14]. Actually, this proposal was originally made by Buettner in 1990 [15]. According to this hypothesis, fast exchange should eliminate this coupling because the β-proton hyperfine coupling of the two conformers would be averaged to a single value. Instead, at 67°C, we see an averaged, highly symmetric spectrum of DMPO/˙OOH with a well-resolved γ-hyperfine coupling constant (Figure 1G). These data support the presence of a hyperfine coupling constant from the γ-proton in the ESR spectrum of DMPO/˙OOH similar to that of the DMPO alkoxyl radical adducts [10].

For the correct simulation of conformational exchange, there are two theoretical approaches: the relaxation matrix method [16] and the modified Block equation method [17]. Although, the modified Block equation method does not consider the effect of possible changes in the nuclear and/or electron spin states during the reaction, it covers the full range of the exchange rate from the rigid limit to fully averaged spectra. Therefore, the modified Block equation method has been chosen to treat the spectra in this study. A program was written in C++ to simulate spectra acquired under 4°C, room temperature (23°C) and 67°C. Two species with the following parameters were used to simulate the spectra at all three temperatures: $a^{N} = 14.14$ G, $a_{\beta}^{H} = 10.90$ G, $a_{\gamma}^{H} = 1.38$ G and $a^{N} = 14.14$ G, $a_{\beta}^{H} = 11.83$ G, $a_{\gamma}^{H} = 0.88$ G. Simulation of the experimental spectra revealed a slow-exchange limit lifetime of 10 μs at 4°C (Figure 2A and B), a conformational lifetime of 0.1 μs at 23°C (Figure 2C and D) and a fast-exchange limit lifetime of 0.001 μs at 67°C (Figure 2E and F) with averaged hyperfine coupling constants of $a^{N} = 14.14$ G, $a_{\beta}^{H} = 11.34$ G and $a_{\gamma}^{H} = 1.22$ G. The room temperature spectrum, Figure 2C, can be simulated as two species, as was the slow-exchange limit spectrum, at 4°C, but with significantly different a_{β}^{H} and a_{γ}^{H}. It is important to note that these partially averaged parameters do not represent distinct species. It is also important to note that the asymmetrical ESR spectrum of DMPO/˙OOH at 4°C may not be at the true slow exchange limit, but the freezing point of water prevented the further lowering of the

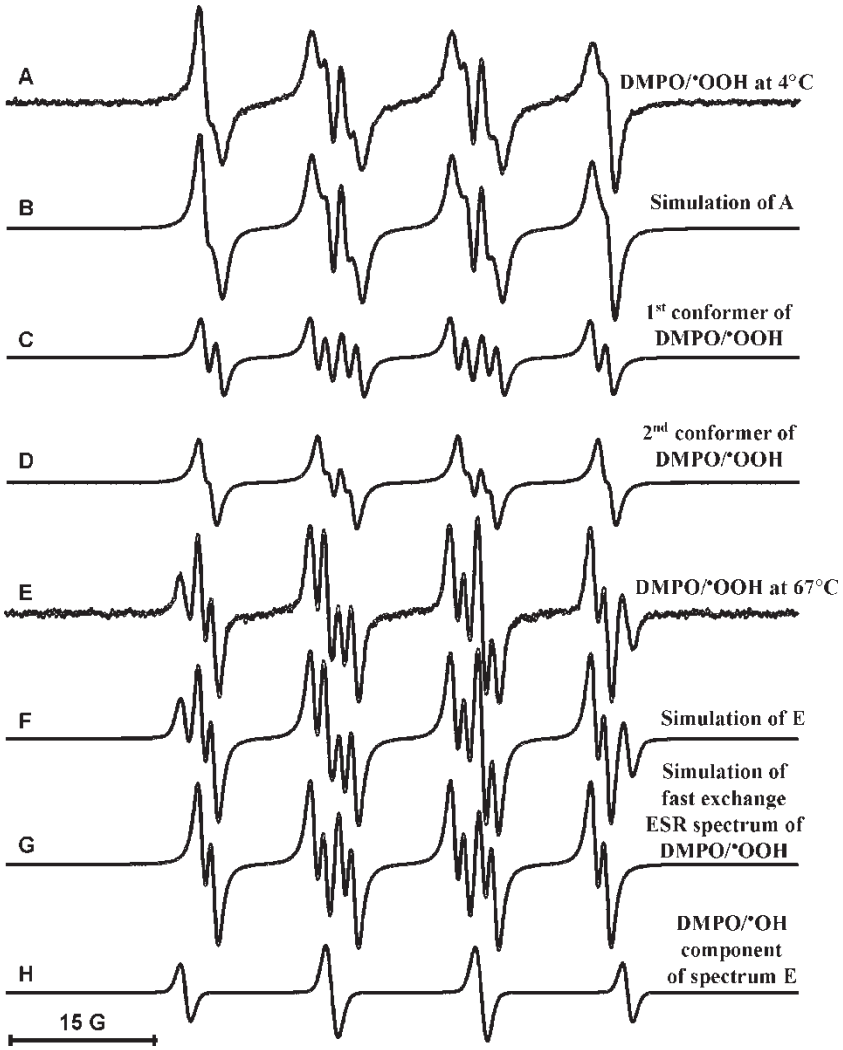

Figure 1. Computer simulation of ESR spectra of DMPO/˙OOH radical adduct at low and high temperature. (A) ESR spectrum of sample obtained by mixing 50 mM DMPO, 10 mU/ml xanthine oxidase and 0.5 mM xanthine at 0.2 ml/min flow at 4°C. (B) Composite computer simulation of spectrum (A). (C) Computer simulation of the ESR spectrum of the first conformer of DMPO/˙OOH in spectrum (A). (D) Computer simulation of the ESR spectrum of the second conformer of DMPO/˙OOH in spectrum (A). (E) ESR spectrum of sample obtained by mixing 50 mM DMPO, 10 mU/ml xanthine oxidase and 0.5 mM xanthine at 0.5 ml/min flow at 67°C. (F) Composite computer simulation of spectrum (E). (G) Computer simulation of the fast exchange ESR spectrum of DMPO/˙OOH in the spectrum (E). (H) Computer simulation of the ESR spectrum of the minor component of DMPO/˙OH in spectrum (E).

temperature without changing the solvent. At 67°C, the symmetrical ESR spectrum is typical of the fast exchange limit between the two conformers.

Effect of temperature on ESR spectra of DEPMPO/˙OOH

The effect of temperature on the ESR spectrum of DEPMPO/˙OOH (Figure 3) was less pronounced but otherwise similar to its effect on the ESR spectrum of DMPO/˙OOH (Figure 1). The asymmetrical ESR lines at low temperature were transformed to lines with higher symmetry at high temperature due to the difference in hyperfine coupling constants of the β-protons of the two DEPMPO/˙OOH conformers (Figure 3A–C), similar to DMPO/˙OOH (Figure 1). However, the superhyperfine structure did not exhibit a temperature dependence (Figure 3D–F). Computer simulation of exchange-modulated ESR spectra of DEPMPO/˙OOH conformers showed a significant effect of conformational exchange on the apparent hyperfine couplings of the respective β-protons: $a_\beta^H =$ 10.6 and 12.0 G (4°C), = 10.6 G and 11.4 G (23°C) and = 11.1 and = 10.9 G (60°C) where the fast exchange limit is approached and the two β-proton hyperfine couplings are nearly equal.

These findings imply that while conformational exchange does indeed affect the ESR spectrum of DEPMPO/˙OOH, it is nevertheless unrelated to the superhyperfine structure. Therefore, we hypothesized that the six-line ESR spectrum with superhyperfine

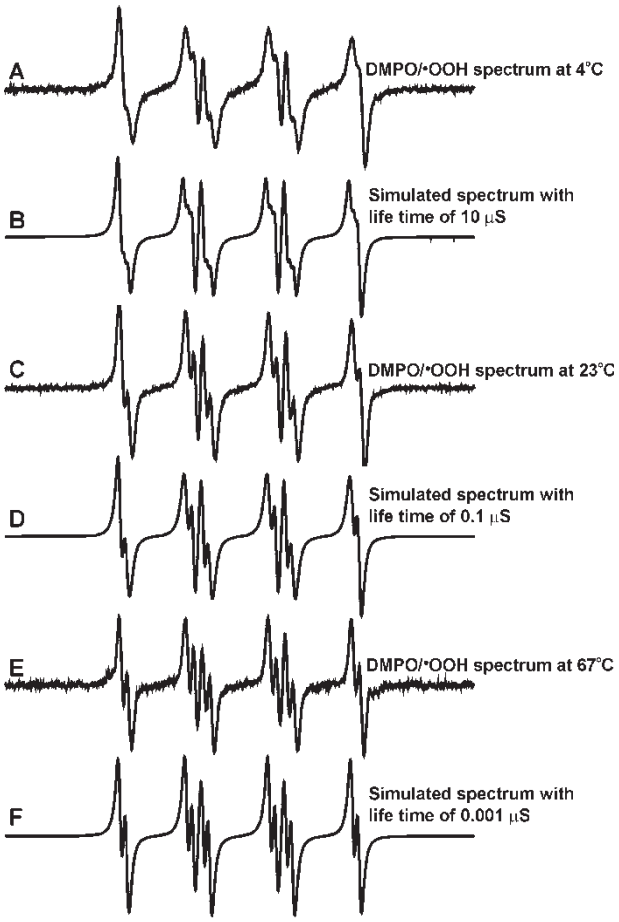

Figure 2. Computer simulations of ESR spectra of DMPO/˙OOH radical adduct using modified Block equation method. (A) Experimental ESR spectrum of DMPO/˙OOH acquired at 4°C. (B) Simulated spectrum with lifetime of 10 μs. (C) Experimental ESR spectrum of DMPO/˙OOH acquired at 23°C. (D) Simulated spectrum with lifetime of 0.1 μs. (E) Experimental ESR spectrum of DMPO/˙OOH acquired at 67°C. (F) Simulated spectrum with lifetime of 0.001 μs. Two conformers of DMPO/˙OOH with the following parameters were used to simulate the spectra: (1) $a^{N} = 14.14$ G, $a^{H}_{\beta} = 10.90$ G and $a^{H}_{\gamma} = 1.38$ G; (2) $a^{N} = 14.14$ G, $a^{H}_{\beta} = 11.83$ G and $a^{H}_{\gamma} = 0.88$ G.

structure can be assigned to a superoxide-derived decomposition product of DEPMPO.

Formation of DEPMPO radical adducts in xanthine oxidase superoxide-generating system

When DEPMPO radical adducts were formed in a xanthine/xanthine oxidase superoxide-generating system and scanned at a modulation amplitude of 1.0 G, a typical ESR spectrum showed a number of structureless lines with a linewidth of approximately one gauss (Figure 4A). When the modulation amplitude was decreased to 0.2 G, superhyperfine structure appeared in a number of the broad lines (Figure 4B). A consecutive scan showed a similar ESR spectrum with slightly smaller intensity (Figure 4C). Subtraction of spectrum C from spectrum B revealed an ESR spectrum consisting of 6 lines with superhyperfine structure (Figure 4D). Formation of all these radical adducts was totally inhibited by superoxide dismutase (Figure 4E).

In order to make sure that the result of subtraction (Figure 4D) was not an artifact due to narrow ESR lines, we repeated this experiment at modulation amplitude 1.0 G (Figure 5). In consecutive scans, the ESR intensity of the DEPMPO radical adducts slowly decayed (Figure 5A–C). A difference spectrum between two consecutive ESR scans revealed an ESR spectrum consisting of 6 lines (Figure 5D) similar to the one observed at low modulation amplitude (Figure 5D) but without the superhyperfine structure because of the overmodulation of the ESR spectra. We propose that this 6-line ESR spectrum with superhyperfine structure belongs to a superoxide-derived decomposition product, DEPMPO/˙X_{OOH}.

The molecule DEPMPO/˙OOH has two chiral centers at the 2nd and 5th positions which produce two chemically distinguishable diastereomers with broad-line ESR spectra. We successfully simulated the experimental spectrum (Figure 6B) using two conformers of the first diastereomer, DEPMPO/˙OOH (39% DEPMPO/˙OOH^{1-1} and 34% DEPMPO/˙OOH^{1-2}); the second diastereomer, 15% DEPMPO/˙OOH; 2% DEPMPO/˙OH; 3% carbon-centered radical adduct, DEPMPO/˙CR_3; and the decomposition product, 7% DEPMPO/˙X_{OOH} (Figure 6, Table I). We suggest that the ESR spectrum previously assigned to DEPMPO/˙OOH consists of two diastereomers of DEPMPO/˙OOH plus the decomposition product DEPMPO/˙X_{OOH} and should be simulated as the sum of 4 species (Figure 6). In order to test this hypothesis, we synthesized an identical DEPMPO-derived species containing superhyperfine structure using nucleophilic addition [18,19].

Nucleophilic synthesis of DEPMPO radical adducts

We used a nucleophilic addition technique previously described for DMPO [18,19] to synthesize DEPMPO-derived radical adducts (Scheme 2). Remarkably, this nucleophilic addition was able to produce a species with the identical ESR superhyperfine structure as was observed in DEPMPO/˙OOH (Figure 6). Computer simulation of the ESR spectrum of this species revealed hyperfine coupling constants for phosphorous (38.9 G), nitrogen (13.1 G) and 6γ–protons (Table I, Figures 4D, 6F and 7C and D). Formation of this species by nucleophilic addition to DEPMPO supports the conclusion that DEPMPO/˙X_{OOH} formed in the xanthine oxidase system is a decomposition product of DEPMPO/˙OOH.

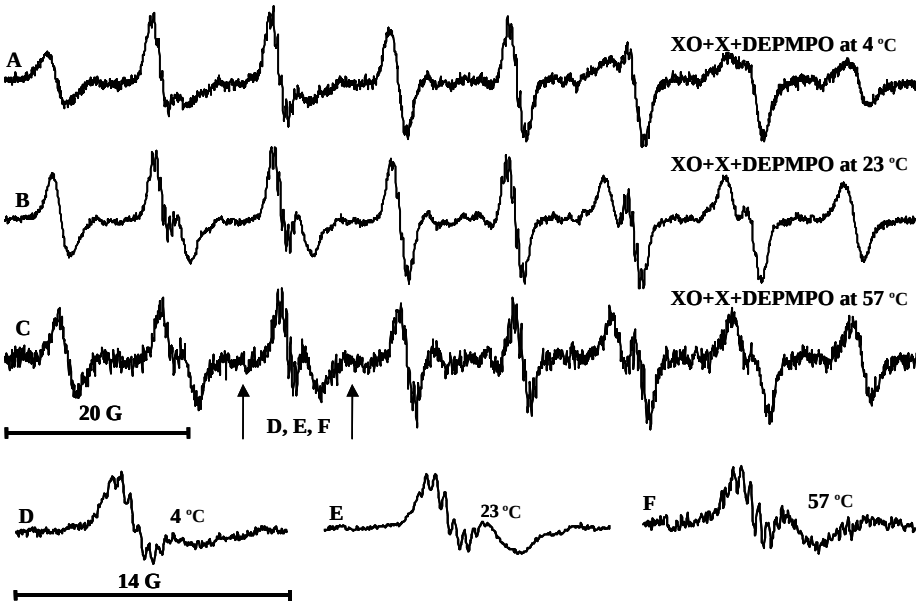

Figure 3. ESR spectra of DEPMPO radical adducts aquired in slow-flow experiments formed by a superoxide-generating system over a temperature range. (A) ESR spectrum of sample obtained by mixing 50 mM DEPMPO, 10 mU/ml xanthine oxidase and 0.5 mM xanthine at 0.2 ml/min flow at 4°C. (B) ESR spectrum of sample obtained by mixing 50 mM DEPMPO, 10 mU/ml xanthine oxidase and 0.5 mM xanthine at 0.2 ml/min flow at 23°C. (C) ESR spectrum of sample obtained by mixing 50 mM DEPMPO, 10 mU/ml xanthine oxidase and 0.5 mM xanthine at 0.5 ml/min flow at 57°C. (D) Components of ESR spectrum (A, 4°C) indicated by arrows. (E) Components of ESR spectrum (B, 23°C) indicated by arrows. (H) Components of ESR spectrum (C, 57°C) indicated by arrows.

Nucleophilic synthesis of DMPO and M4PO radical adducts

Superhyperfine structure in the ESR spectra has previously been reported for radical adducts of decomposition products derived from the spin-trap DMPO as a result of nucleophilic addition of water in the presence of H_2O_2 [19]. Therefore, in order to clarify the structure of the decomposition product DEPMPO/$^{\cdot}X_{OOH}$, we synthesized radical adducts of the similar spin-traps DMPO and M4PO (Scheme 1) by addition of water (Scheme 2). Nucleophilic synthesis with DMPO revealed a species with superhyperfine structure in the ESR spectrum (Figure 8) previously assigned as DMPO/$^{\cdot}(OH)_2$ [19]. This DMPO-derived species has no β-proton, and the superhyperfine structure can be simulated by hyperfine coupling constants from three γ-protons, 0.8, 1.14 and 2.32 G.

The spin-trap M4PO has a chemical structure similar to DEPMPO and DMPO, with two methyl

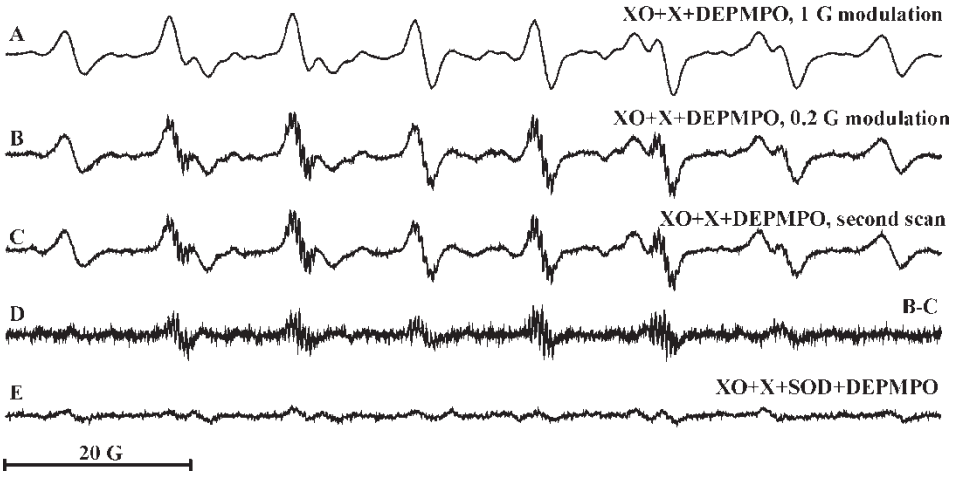

Figure 4. Formation of DEPMPO radical adducts in xanthine oxidase superoxide-generating system. (A) ESR spectrum of 50 mM DEPMPO, 10 mU/ml xanthine oxidase and 0.5 mM xanthine scanned at modulation amplitude 1 G. (B) ESR spectrum of 50 mM DEPMPO, 10 mU/ml xanthine oxidase and 0.5 mM xanthine scanned at modulation amplitude 0.2 G. (C) Same as (B) but 5 min later. (D) Subtraction of spectrum (C) from spectrum (B). (E) ESR spectrum of 50 mM DEPMPO, 10 mU/ml xanthine oxidase and 0.5 mM xanthine plus 50 U/ml SOD.

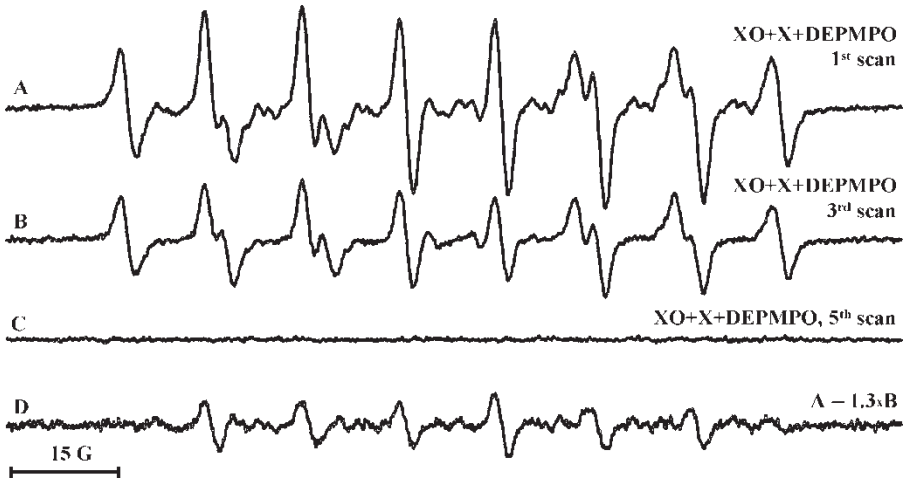

Figure 5. ESR spectra of DEPMPO radical adducts in superoxide generating system with modulation 1 G. (A) ESR spectrum of 50 mM DEPMPO, 10 mU/ml xanthine oxidase and 0.5 mM xanthine scanned at modulation amplitude 1 G. (B) Same as (A) but two scans later. (C) Same as (B) but four scans later. (D) Subtraction of spectrum (B) (times 1.3) from spectrum (A).

groups substituted for the γ-protons at the 3rd position (Scheme 1). Nucleophilic synthesis with Fe^{3+} (Scheme 3) produced an M4PO/˙OH radical adduct (Figure 9A and B: $a^{N} = 15.24$ G and $a^{H}_{\beta} = 16.63$ G). In the presence of 10 mM $FeCl_3$ and 100 mM H_2O_2, M4PO formed a nitroxide with a very small nitrogen hyperfine coupling constant of 6.90 G, which was assigned as M4POX (Figure 9C and D). Nucleophilic addition with a higher concentration of M4PO revealed a new species that had no β-proton and no superhyperfine structure. It had a nitrogen hyperfine coupling constant of 17.72 G, much higher than the nitrogen coupling constant of the DMPO-derived species with superhyperfine structure in the ESR spectrum. Therefore, nucleophilic synthesis gave different products for DMPO and M4PO. This

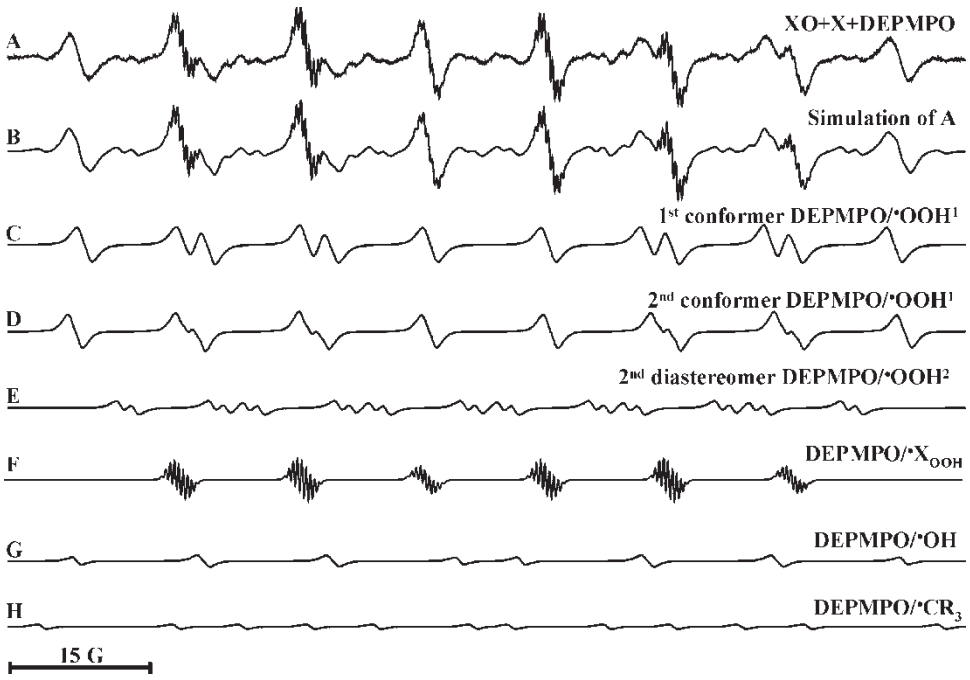

Figure 6. Computer analysis of DEPMPO radical adducts formed in superoxide-generating system. (A) ESR spectrum of sample obtained by mixing of 50 mM DEPMPO, 10 mU/ml xanthine oxidase and 0.5 mM xanthine at slow flow (0.2 ml/min) and scanned at modulation amplitude 0.2 G. (B) Composite computer simulation of spectrum (A). (C) Computer simulation of the ESR spectrum of the first conformer of the first diastereomer of DEPMPO/˙OOH in spectrum (A). (D) Computer simulation of the ESR spectrum of the second conformer of the first diastereomer of DEPMPO/˙OOH in spectrum (A). (E) Computer simulation of the ESR spectrum of the second diastereomer of DEPMPO/˙OOH in spectrum (A). (F) Computer simulation of the ESR spectrum of decomposition product DEPMPO/X_{OOH} in spectrum (A). (G) Computer simulation of the ESR spectrum of DEPMPO/˙OH in spectrum (A). (H) Computer simulation of the ESR spectrum of carbon-centered radical adduct DEPMPO/˙CR_3 in spectrum (A).

Table I. Hyperfine coupling constants of DEPMPO radical adducts (G).

Radical adduct	N	H_β	H_{CH_3}	H^3_γ	H^3_γ	H^4_γ	H^4_γ	^{31}P	^{17}O
DEPMPO/˙OH	13.97	13.11						46.50	4.07
	13.98	13.12						47.64	4.08
DEPMPO/˙OOH[1] conformers	13.12	10.57		0.74				49.40	5.12
	13.12	11.42		0.76				50.58	4.86
DEPMPO/˙OOH[2]	13.40	9.81		1.50				40.47	
DEPMPO/$\dot{X}_{OOH}$	13.09	–	0.45	0.98	–	0.86	0.42	38.98	

difference is likely to be associated with the absence of γ- protons at the 3rd position in the structure of M4PO. Thus, γ- protons at the 3rd position are likely to be involved in the formation of the decomposition product DEPMPO/$\dot{X}_{OOH}$.

Analysis of ESR spectrum of isotope-labeled DEPMPO/^{17}OOH

Isotopic substitution is a very useful technique for the correct assignment of radical adducts, helping to distinguish alkoxyl and peroxyl radical adducts as well as facilitating correct assignment of hyperfine coupling constants [20]. We used $H_2^{17}O$ to synthesize DEPMPO/^{17}OH by nucleophilic addition and $^{17}O_2$ to generate the DEPMPO/^{17}OOH radical adduct with the xanthine oxidase system.

DEPMPO/^{16}OH can be formed by the nucleophilic addition of water to DEPMPO (Figure 10A). When isotope-labeled water, $H_2^{17}O$ (45%), was substituted, the resulting ESR spectrum consisted of 45% DEPMPO/^{17}OH and 55% DEPMPO/^{16}OH (Figure 10B and C). The DEPMPO/^{16}OH (Figure 10A) component (55%) was subtracted from the composite

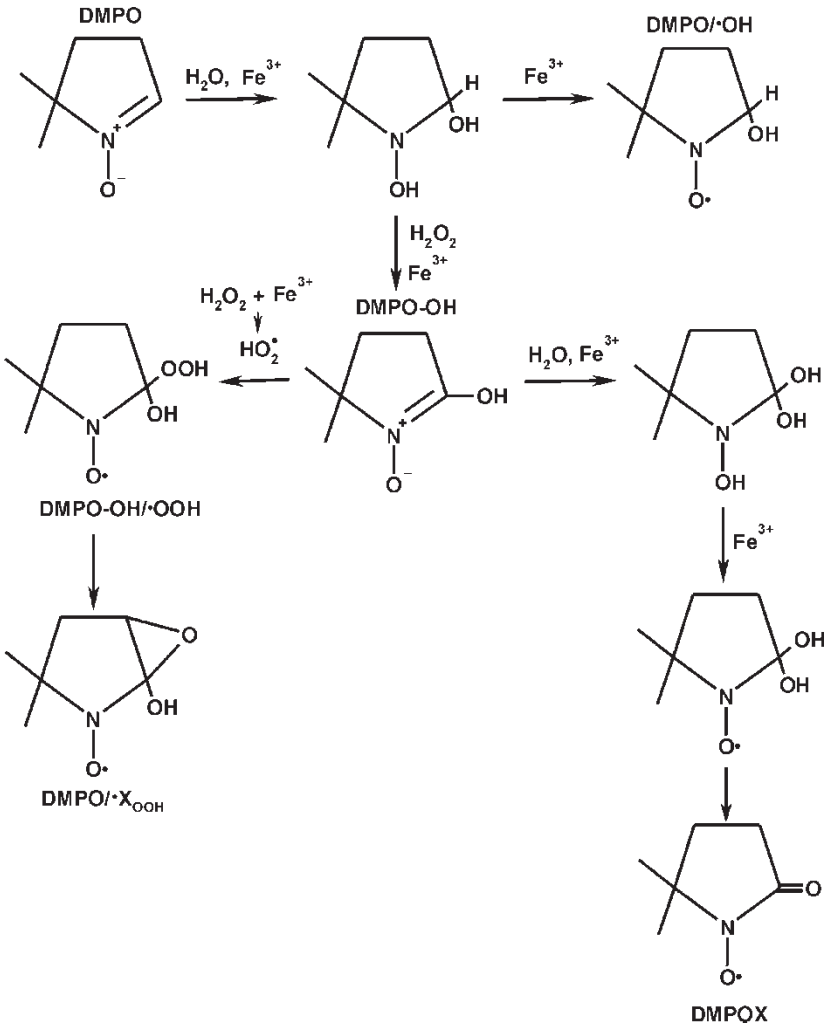

Scheme 2. Synthesis of the DMPO radical adducts by nucleophilic addition of water to DMPO.

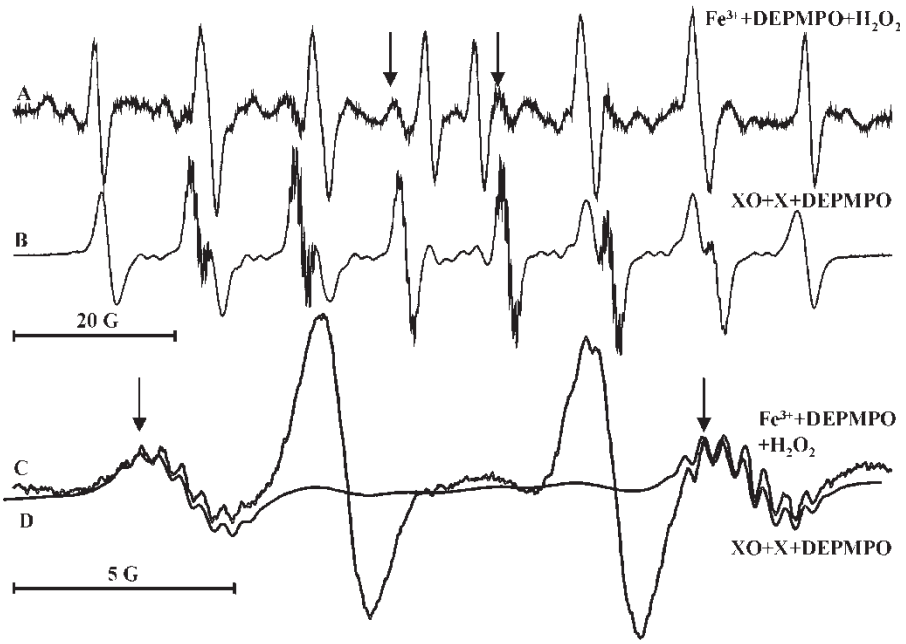

Figure 7. ESR spectra of DEPMPO radical adducts formed in xanthine oxidase system and by nucleophilic addition of water in the presence of H_2O_2. (A) ESR spectrum of water solution of 50 mM DEPMPO with 0.5 mM $FeCl_3$ in the presence of 50 mM H_2O_2. (B) ESR spectrum of sample obtained by mixing 50 mM DEPMPO, 10 mU/ml xanthine oxidase and 0.5 mM xanthine at 0.2 ml/min flow. (C) Components of ESR spectrum (A) indicated by arrows. (D) Components of ESR spectrum (B) overlaid with spectrum (A) indicated by arrows.

spectrum (Figure 10B) to reveal the DEPMPO/^{17}OH radical adduct (Figure 11D and E). The hyperfine coupling constant for ^{17}O in DEPMPO/^{17}OH was 4.07 G (Table I).

When the xanthine oxidase superoxide-generating system was run with $^{17}O_2$, the ESR spectrum exhibited a hyperfine coupling constant from ^{17}O (Figure 11A). This experimental ESR spectrum could

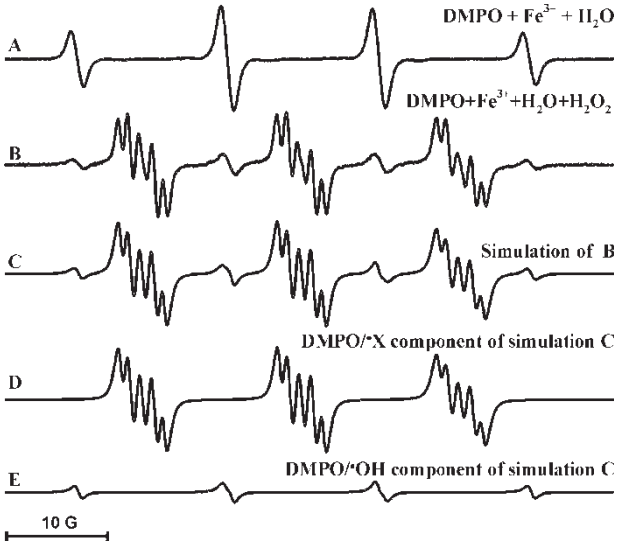

Figure 8. Synthesis of DMPO-derived nitroxides with hyperfine structure in the ESR spectrum. (A) ESR spectrum of water solution of 50 mM DMPO with 0.5 mM $FeCl_3$. (B) ESR spectrum of water solution of 50 mM DMPO with 0.1 mM $FeCl_3$ in the presence of 50 mM H_2O_2. (C) Composite computer simulation of spectrum (B). (D) Computer simulation of the ESR spectrum of the DMPO-derived decomposition product. (E) Computer simulation of the ESR spectrum of DEPMPO/˙OH in spectrum (B).

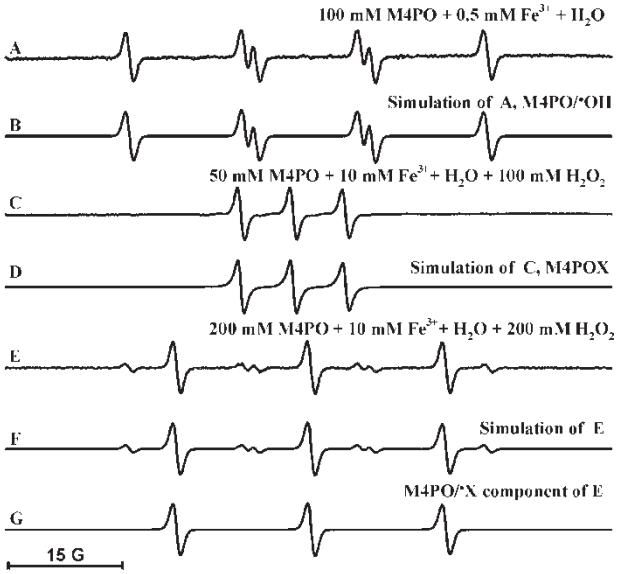

Figure 9. Synthesis of M4PO-derived nitroxides by nucleophilic addition. (A) ESR spectrum of water solution of 50 mM M4PO with 0.5 mM $FeCl_3$. (B) Computer simulation of spectrum (A). (C) ESR spectrum of water solution of 50 mM M4PO with 10 mM $FeCl_3$ in the presence of 100 mM H_2O_2. (D) Computer simulation of spectrum (C). (E) ESR spectrum of water solution of 200 mM M4PO with 10 mM $FeCl_3$ in the presence of 200 mM H_2O_2. (F) Composite computer simulation of spectrum (E). (G) Computer simulation of the ESR spectrum of M4PO-derived decomposition product.

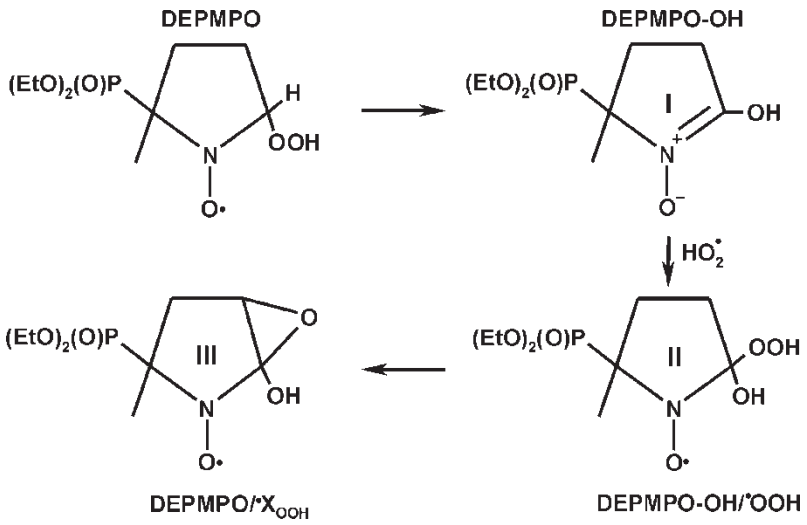

Scheme 3. Proposed scheme of decomposition of DEPMPO-superoxide radical adduct.

be simulated as a combination of two conformers of DEPMPO/$^{\cdot 17}$OOH and two conformers of DEPMPO/$^{\cdot 16}$OOH (Figure 11B–F). Interestingly, despite numerous attempts we never observed ESR spectra with $^{17}O_2$ superhyperfine structure and, therefore, the ^{17}O spectra can be simulated without the decomposition product DEPMPO/$^{\bullet}X_{OOH}$. The ^{17}O hyperfine-coupling constants of conformers of DEPMPO/$^{\cdot 17}$OOH were 4.86 G and 5.14 G, quite distinct from those of DEPMPO/$^{\cdot 17}$OH (Table I).

Discussion

Unfortunately, the interpretation of ESR spectra of DEPMPO radical adducts is difficult. The spectra are complicated by the presence of diastereomers and may be obscured by the presence of additional radical adducts.

We have shown how to exploit the difference in stability of the radical adducts to separate specific radical adducts by subtracting consecutive ESR spectra. We have also demonstrated that the hyperfine structure present in the ESR spectra of DEPMPO superoxide radical adducts is the product of decomposition of the superoxide radical adducts. Formation of these decomposition products was confirmed by temperature independence (Figures 1–3), subtraction of ESR spectra (Figures 4 and 5), nucleophilic synthesis of DMPO and M4PO analogs (Figures 7–9) and ^{17}O-labeling (Figures 10 and 11).

The mechanism of formation of these decomposition products is not clear. The similarity of the

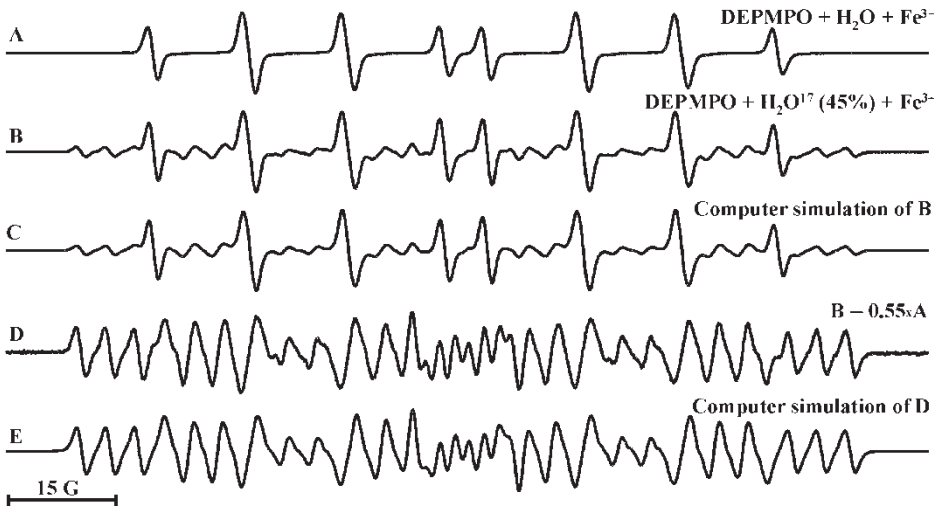

Figure 10. Analysis of ESR spectrum of DEPMPO/$^{\cdot 17}$OH radical adduct. (A) ESR spectrum of N_2-bubbled H_2O solution of 50 mM DEPMPO with 0.2 mM $FeCl_3$. (B) ESR spectrum of N_2-bubbled $H_2^{17}O$ (45-atom %) solution of 50 mM DEPMPO with 0.2 mM $FeCl_3$. (C) Composite computer simulation of spectrum (B). (D) ESR spectrum obtained by the subtraction of spectrum (A) from spectrum (B). (E) Composite computer simulation of spectrum (D).

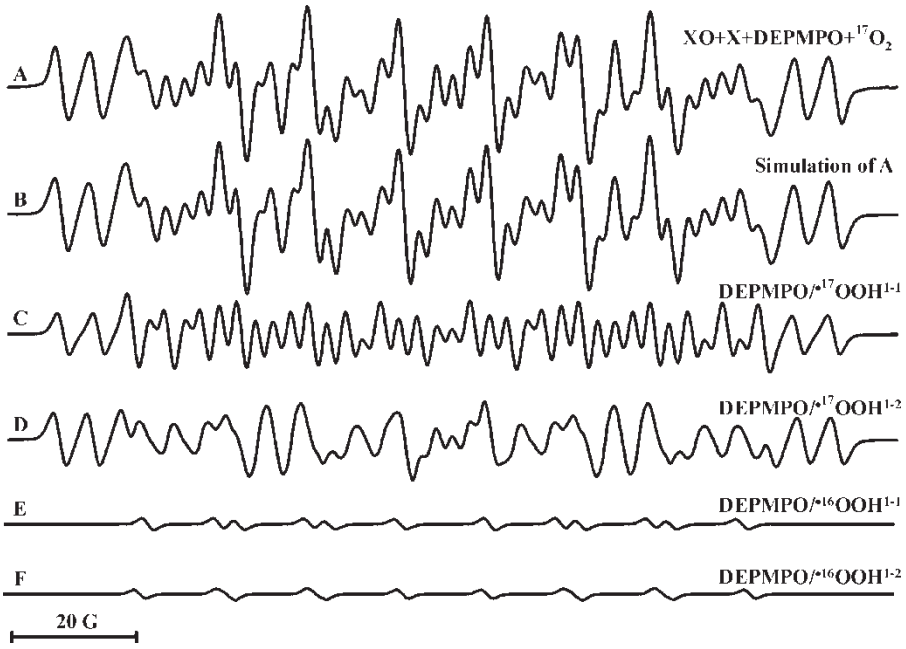

Figure 11. Computer analysis of DEPMPO radical adducts formed in ^{17}O-labeled superoxide-generating system. (A) ESR spectrum of $^{17}O_2$-bubbled (85-atom %) solution with 50 mM DEPMPO, 10 mU/ml xanthine oxidase and 0.5 mM xanthine scanned at modulation amplitude 0.2 G. (B) Composite computer simulation of spectrum (A). (C) Computer simulation of the ESR spectrum of the first conformer of DEPMPO/^{17}OOH in spectrum (A). (D) Computer simulation of the ESR spectrum of the second conformer of DEPMPO/^{17}OOH in spectrum (A). (E) Computer simulation of the ESR spectrum of the first conformer of DEPMPO/^{16}OOH in spectrum (A). (F) Computer simulation of the ESR spectrum of the second conformer of DEPMPO/^{16}OOH in spectrum (A).

DEPMPO decomposition product with superhyperfine structure to the one from DMPO suggests a common mechanism for both spin-traps. The formation of a DMPO-derived nitroxide whose ESR spectrum contains hyperfine structure has been described by Makino et al. [19] who suggested that the initial formation of the DMPO-OH nitrone (Scheme 2) was followed by the addition of a second hydroxyl radical, forming DMPO/$^{\bullet}(OH)_2$ as a final product. However, this type of chemical structure is generally very unstable and will be transformed to the ketone form DMPOX, a stable nitroxide with a very characteristic ESR spectrum. We found that under varying experimental conditions, either the DMPO-derived nitroxide with hyperfine structure or DMPOX was formed. Therefore, these two products may be formed by different mechanisms. DMPO-OH nitrone could react with superoxide radical formed by the oxidation of H_2O_2 with Fe^{3+}, which would lead to the formation of DMPO-OH/$^{\bullet}$OOH. The absence of a nitroxide product with superfine structure from M4PO may suggest involvement of the proton at the third position in the formation of an epoxy-derivative during the decay of DMPO-OH/$^{\bullet}$OOH radical adduct (Scheme 2). This adduct has no β-proton and may have hyperfine coupling from three γ-protons at the third and fourth positions (Figure 4D).

Recently, it was reported that DEPMPO-OH nitrone is one of the major products of DEPMPO/$^{\bullet}$OOH decomposition [21]. Therefore, we can suggest formation of DEPMPO/$^{\bullet}X_{OOH}$ via DEPMPO-OH nitrone similar to DMPO (Scheme 3). According to this scheme, DEPMPO/$^{\bullet}X_{OOH}$ can be a spin-trapping product of a secondary nitrone formed during decomposition of DEPMPO/$^{\bullet}$OOH.

This paper also supports the presence of two conformers of the DEPMPO/$^{\bullet}$OOH radical adduct. However, conformational exchange is not responsible for the appearance of superhyperfine structure in some lines as was previously suggested [8,9].

Acknowledgements

We thank Ms Mary Mason for helping in the preparation of this article.

References

[1] Liochev SI, Fridovich I. Superoxide and iron: Partners in crime. IUBMB Life 1999;48:157–161.
[2] Visioli F, Galli C. Evaluating oxidation processes in relation to cardiovascular disease: A current review of oxidant/antioxidant methodology. Nutr Metab Cardiovasc Dis 1997;7:459–466.
[3] Janzen EG. Spin trapping. Acc Chem Res 1971;4:31–40.
[4] Janzen EG, Haire DL. Two decades of spin trapping. Adv Free Radic Chem 1990;1:253–295.
[5] Buettner GR, Mason RP. Spin-trapping methods for detecting superoxide and hydroxyl free radicals *in vitro* and *in vivo*. Methods Enzymol 1990;186:127–133.

[6] Buettner GR, Mason RP. Spin-trapping methods for detecting superoxide and hydroxyl free radicals *in vitro* and *in vivo*. In: Cutler RG, Rodriguez H, editors. Critical reviews of oxidative stress and aging: Advances in basic science, diagnostics and intervention. New Jersey: World Scientific; 2002. p 27–38.

[7] Frejaville C, Karoui H, Tuccio B, Le Moigne F, Culcasi M, Pietri S, Lauricella R, Tordo P. 5-Diethoxyphosphoryl-5-methyl-1-pyrroline *N*-oxide (DEPMPO)—A new phosphorylated nitrone for the efficient *in vitro* and *in vivo* spin trapping of oxygen-centred radicals. J Chem Soc Chem Commun 1994;15:1793–1794.

[8] Frejaville C, Karoui H, Tuccio B, Le Moigne F, Culcasi M, Pietri S, Lauricella R, Tordo P. 5-(Diethoxyphosphoryl)-5-methyl-1-pyrroline *N*-oxide—A new efficient phosphorylated nitrone for the *in vitro* and *in vivo* spin trapping of oxygen-centered radicals. J Med Chem 1995;38:258–265.

[9] Rockenbauer A, Korecz L. Automatic computer simulations of ESR spectra. Appl Magn Reson 1996;10:29–43.

[10] Dikalov SI, Mason RP. Spin trapping of polyunsaturated fatty acid-derived peroxyl radicals: Reassignment to alkoxyl radical adducts. Free Radic Biol Med 2001;30:187–197.

[11] Fridovich I. Xanthine oxidase. In: Greenwald RA, editor. CRC handbook of methods for oxygen radical research. New York: CRC Press; 1985. p 51–53.

[12] Fridovich I. Cytochrome *c*. In: Greenwald RA, editor. CRC handbook of methods for oxygen radical research. New York: CRC Press; 1985. p 121–122.

[13] Duling DR. Simulation of multiple isotropic spin-trap EPR spectra. J Magn Res Series B 1994;104:105–110.

[14] Rosen GM, Beselman A, Tsai P, Pou S, Mailer C, Ichikawa K, Robinson BH, Nielsen R, Haplern HJ, MacKerell AD, Jr.. Influence of conformation on the EPR spectrum of 5,5-dimethyl-1-hydroperoxy-1-pyrrolidinyloxyl: A spin trapped adduct of superoxide. J Org Chem 2004;69:1321–1330.

[15] Buettner GR. On the reaction of superoxide with DMPO/-˙OOH. Free Radic Res Commun 1990;10:11–15.

[16] Freed JH, Fraenkel GK. Alternating linewidths and related phenomena in the electron spin resonance spectra of nitro-substituted benzene anions. J Chem Phys 1964;41:699–716.

[17] Sullivan PD, Bolton JR. The alternating linewidth effect. Advan Magn Reson 1970;4:39–85.

[18] Hanna PM, Chamulitrat W, Mason RP. When are metal ion-dependent hydroxyl and alkoxyl radical adducts of 5,5-dimethyl-1-pyrroline *N*-oxide artifacts? Arch Biochem Biophys 1992;296:640–644.

[19] Makino K, Hagi A, Ide H, Murakami A, Nishi M. Mechanistic studies on the formation of aminoxyl radicals from 5,5-dimethyl-1-pyrroline-*N*-oxide in Fenton systems. Characterization of key precursors giving rise to background ESR signals. Can J Chem 1992;70:2818–2827.

[20] Dikalov SI, Mason RP. Reassignment of organic peroxyl radical adducts. Free Radic Biol Med 1999;27:864–872.

[21] Khramtsov V, Berliner LJ, Clanton TL. NMR spin trapping: Detection of free radical reactions using a phosphorus-containing nitrone spin trap. Magn Reson Med 1999; 42:228–234.